TU Delft

Delft University of Technology

Document Version
Final published version

Licence
CC BY

Citation (APA)
de Wind, J. A. J., Alpizar Castillo, J. J., Visser, J., & Ramirez Elizondo, L. M. (2025). An In-Depth Analysis of Residential E-Cooling Demand in the Netherlands. *Case Studies in Thermal Engineering*, *73*. https://doi.org/10.1016/j.csite.2025.106469

Important note
To cite this publication, please use the final published version (if applicable).
Please check the document version above.

Copyright
In case the licence states “Dutch Copyright Act (Article 25fa)”, this publication was made available Green Open Access via the TU Delft Institutional Repository pursuant to Dutch Copyright Act (Article 25fa, the Taverne amendment). This provision does not affect copyright ownership.
Unless copyright is transferred by contract or statute, it remains with the copyright holder.

Sharing and reuse
Other than for strictly personal use, it is not permitted to download, forward or distribute the text or part of it, without the consent of the author(s) and/or copyright holder(s), unless the work is under an open content license such as Creative Commons.

Takedown policy
Please contact us and provide details if you believe this document breaches copyrights.
We will remove access to the work immediately and investigate your claim.

This work is downloaded from Delft University of Technology.

Case Studies in Thermal Engineering 73 (2025) 106469

Contents lists available at ScienceDirect

Case Studies in Thermal Engineering

journal homepage: www.elsevier.com/locate/csite

An in-depth analysis of residential E-cooling demand in The Netherlands

Jim de Wind [a,b], Joel Alpízar-Castillo [a,*], Julian Visser [b], Laura Ramírez-Elizondo [a]

[a] DC Systems, Energy Conversion and Storage Group, Delft University of Technology, Mekelweg 6, Delft, 2628 CD, Zuid Holland, The Netherlands

[b] Eneco, P.O. 8202, Rotterdam, 3009AE, Zuid Holland, The Netherlands

GRAPHICAL ABSTRACT

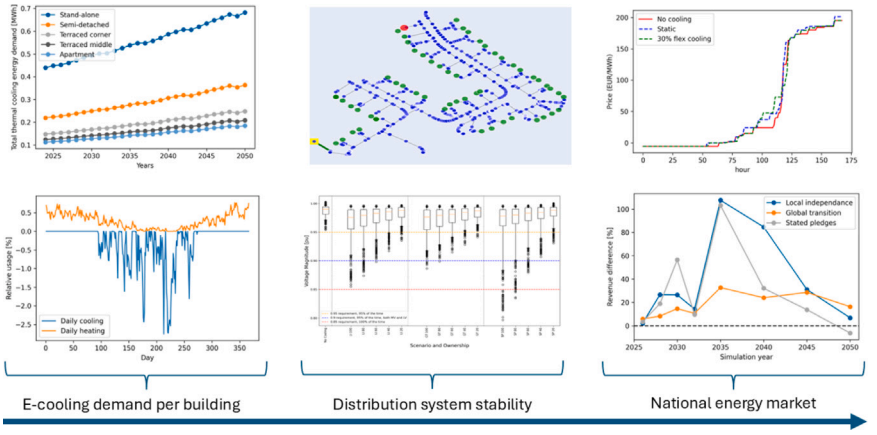

HIGHLIGHTS

- The cooling energy demand will amount to 0.2–0.4 TWh annually in The Netherlands by 2050.
- Residential cooling can amount to 2.5% of the yearly cooling demand on a single day.
- Adoptions of over 40% of heat pumps cause voltage instability in low-voltage networks.
- The demand for e-cooling might increase prices in the Dutch energy market during heat waves.
- The demand for e-cooling increases revenue for RES generators and decreases it for batteries.

ARTICLE INFO

Keywords:
Electric cooling

ABSTRACT

The magnitude and effect of residential E-cooling demand on the Dutch energy market have not been studied in the literature. However, due to rising temperatures and the increase in the

* Corresponding author.
E-mail address: J.J.AlpizarCastillo@tudelft.nl (J. Alpízar-Castillo).

https://doi.org/10.1016/j.csite.2025.106469
Received 1 May 2025; Received in revised form 27 May 2025; Accepted 5 June 2025
Available online 23 June 2025
2214-157X/© 2025 The Authors. Published by Elsevier Ltd. This is an open access article under the CC BY license (http://creativecommons.org/licenses/by/4.0/).

Heat pump
Energy market

adoption of heat pumps, the effects of residential e-cooling demand are expected to rise sharply in the upcoming decades. First, a thermodynamic model of different Dutch residential buildings described the magnitude and patterns of residential E-cooling. Second, the effects of E-cooling on the distribution network were tested using the IEEE 906-bus European LV network. Third, a country-wide simulation of the effect of residential E-cooling on the energy market was done in Plexos© from 2025 to 2050. The results showed a doubling of the cooling demand between 2025 and 2030 and a maximum annual cooling demand of approximately 0.4 TWh. In addition, it was shown how the demand for residential cooling could decrease local power quality when more than 40 % of households actively cool their houses simultaneously, increasing network costs. Finally, it was also proven how power prices could increase due to higher demand and how revenue for specific generation components could double or decrease by 20% during heat waves when accounting for residential E-cooling demand.

Nomenclature

Abbreviations

CBS	Dutch Central Bureau of Statistics
COP	Coefficient of performance
E-cooling	Electric cooling
GT	Global transition
HP	Heat pump
KNMI	Royal Dutch Meteorological Institute
LI	Local independence
SP	Stated pledges
WWR	Window-to-wall ratio

1. Introduction

The temperature in the Netherlands is rapidly increasing due to global carbon emissions. The climate warming stripes provided by [1] reveal a notable increase in average yearly temperature, particularly from the 1990s, changing from temperatures below 9 °C until the 1940s to over 11 °C by 2020. By 2016, the residential spatial heating demand in the Netherlands amounted to 85 TWh/year compared to 0.2 TWh/year of spatial cooling demand [2]. However, due to the aforementioned warming of the Dutch climate, it can be expected that the spatial heating demand will decrease. Opposed to this, the spatial cooling demand, currently very small, will likely increase significantly. To solve this, many households are buying heat pumps to satisfy their cooling demand.

Currently, around 17% of Dutch households have air–air heat pumps (HPs) [3]. The absolute amount of air–water-based and air–air-based heat pumps in the Netherlands has increased exponentially in the last five years, as shown in Fig. 1. In particular, the number of air–air-based heat pumps, which often can be used for electric cooling (E-cooling), is increasing at a rapid rate. However, little is known about the magnitude of future cooling demand and its impact on the Dutch electricity grid nor on the Dutch energy market. Some studies have been conducted to uncover the magnitude of future cooling demand. However, these were performed using questionnaires [4] and are not based on physical data. Other reports are based mainly on USA data that are not necessarily transferable to the Netherlands [5]. In addition, some papers on this subject oversimplified the effects of solar irradiance or assumed a single-building type, creating an oversimplified model [6,7], instead of considering the infrastructure diversity for residential buildings, such as individual houses, (semi-)detached houses, terraced houses, or apartment buildings. At the time of writing and to the best knowledge of the authors, no single study has been performed on the magnitude of future Dutch residential spatial cooling demand and the effects on the Dutch grid.

1.1. Relevant literature

The energy transition aims to minimize the usage of fossil-fuels from the energy matrix. From a thermal comfort perspective at the residential level, the heating demand has been traditionally supplied by gas boilers, while the cooling demand is supplied by electric air conditioning systems. Also, there are regions typically supply only one of those demands at the residential level. For instance, Northern Europe households rarely have cooling systems, as the frequency of high temperatures is not enough to justify the acquisition of such systems [2]. Nevertheless, the global warming and the heat island effect has consistently increased the temperatures in cities [8]. In addition, heat pumps have been widely accepted as electric heating devices, which can also meet cooling demands, giving the option to also cool indoor spaces, creating a new energy demand in some markets.

From a modelling perspective, the same models used to estimate the heating demand can be used for cooling demand, given they consider the indoor, outdoor and desired temperature. In this regard, there are many works in the literature focused in estimating the thermal loads. To elucidate in the most relevant variables required to construct building thermal models, [9] used

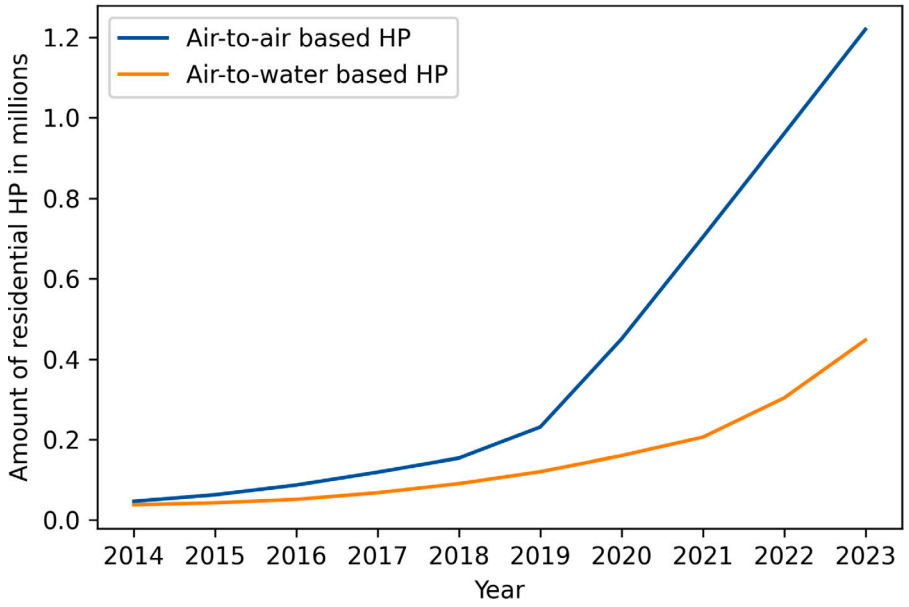

Fig. 1. The absolute amount of two types of heat pumps in the residential sector in the Netherlands according to the Dutch Central Bureau for Statistics [3].

model-based recursive partitioning to create decision tree models to understand the relevance of different variables associated with residential energy consumption. The model was trained using data from the 2020 Residential Energy Consumption Survey, concluding that, for heating and cooling, the type of climate, the construction year, the insulation (particularly in windows) and the type of heating/cooling system are the most influential variables. Therefore, a good model to estimate the thermal load, must consider some, if not all, of those variables to create a realistic representation of the thermal demand. Some analytical models, such as the one in [10] provide an open-access mathematical framework in Python to model a residential building, based on the thermodynamic interactions between indoor and outdoor and a geometric description of the building. However, their work focused only in heating, and neglected phenomena that would eventually increase the cooling demand, for instance, heating through the windows due to radiation. Similar analytical methods, based on the heat balance method proposed by the ASHRAE, are used in commercial software such as EnergyPlus© and TRNSYS©to create representative buildings, but without providing a lot of flexibility to make detailed changes in the model [11].

Other non-analytical methods have been proposed in the literature to avoid describing the buildings from a geometric and thermodynamic perspective using directly load demand. In [12], for instance, a complex neural network was used to forecast multi-energy loads for the next hour, in particular heating, cooling and electric loads, using data from the Arizona State University's Tempe campus, achieving mean absolute percentage errors between 1.7% and 4.7%. However, three years of historical data of the load consumption and meteorological data was required to train the model. Similarly, [13] used Improved complete ensemble empirical mode decomposition with adaptive noise, combined with fuzzy dispersion entropy, over-zero rate, successive variational mode decomposition, multiple linear regression, temporal convolutional network and multi-head attention to predict electric, cooling and heating loads, using data for the year 2020, also from the Arizona State University's Tempe campus, and weather data from the Phoenix International Airport. Their method was capable of predicting 9 h ahead with a mean absolute percentage error between 0.85% and 1.95%. In [14], a long short-term memory network model, combined with a convolutional neural network model and harmony search optimized light gradient boosting machine was used to predict the electric, heating and cooling demand. The load data used was from the Arizona State University's Tempe campus and the meteorological data was retrieved from the National Renewable Energy Laboratory of the United States, achieving a mean absolute percentage error of 4.38%.

With respect to the electric component of the electric cooling systems, the literature focuses on optimizing the utilization of the heating or cooling systems based on price, such as [15,16]. On the local perspective, some works have studied alternatives to generate locally to compensate for the additional energy demand required for electric cooling with renewable sources. For instance, [17] used survey data from the USA Energy Information Administration to size systems capable of compensating the demand requirements of space cooling in commercial buildings between 90^2 and 900 m^2 with PV systems. Their conclusions suggest that, energy-wise, the compensation is possible, but there is a mismatch between the generation and the cooling demand, which can create challenges for the distribution networks. Considering that the operation principle of electric cooling is comparable to the electric heating, some works have focused on studying the effects of heat pumps in the distribution networks. For instance, [18] compared the effect of aggregated and non-aggregated under different adoption scenarios in a real low-voltage 301-node distribution network in the Netherlands. For the non-aggregated scenario, the network can accommodate adoptions between 20% and 40%, while the aggregated scenarios surpass the 60%. These results are consistent with other works, which suggest that major reinforcements are

required for higher adoptions of heat pumps used to heat during winter, but that can also supply cooling demand during summer. For example, [19] concluded that, in Germany, energy sharing strategies can reduce energy costs by up to 80% and transformer loading by up to 68%, and [20] demonstrated that residential multi-carrier systems can participate in the congestion management at low-voltage distribution networks. However, deeper analysis are still needed from a voltage stability point of view.

Despite the yearly energy demand for electric cooling might not be considerable in many countries in Northern Europe, where this research is focused, it is worth mentioning that most of that cooling demand happens in short time frames, which might affect the energy market. The work in [21] show that demand profiles with high peaks in summer can increase costs by 8% in the European energy market, and [22] demonstrated that OECD countries have consistently high higher cooling electricity requirements. Considering that the cooling demand would be concentrated in summer, a potential effect on the energy market might arise.

1.2. Contribution

Based on the literature review done in Section 1.1, the research gaps found are:

- many studies focus on the effects of residential heating electrification as part of the energy transition, however, little attention is given to the effect cooling electrification, particularly in Northern Europe,
- many studies assume all houses equal instead of considering or approximating the variable sizes, configurations and characteristics present in a region or country, or use direct load to create non-analytical models, which is hard to acquire and generalize for different types of buildings, and
- very few studies have considered the effect of electric cooling into the energy market, given the very low magnitude in the yearly basis compared to other demands; nonetheless, the cooling demand is concentrated in shorter periods per year, increasing the relative share of the energy demand for cooling.

In this work, we modelled different types of houses and the proportion of each type in the overall Dutch house market, and considered three different adoption scenarios of electric cooling. Therefore, the contributions of this paper are

- an estimation of the energy demand for residential electric cooling in the Netherlands, for three adoption scenarios, until 2050, considering the different types of residential buildings,
- a study on the impact of residential electric cooling on the low-voltage distribution network for three different adoption scenarios and penetration levels, and
- an analysis on the impact of the increased energy demand caused by residential electric cooling in the Dutch energy market for three adoption scenarios, including revenue changes in solar generation and battery storage.

To achieve the previous contributions, the following methodology was used. First, we conducted a study on the current housing stock in the Netherlands to determine a more accurate distribution of the types of residential building. Then, we adapted an existing analytical model to account for cooling demand the four main types of buildings in the Netherlands; this way, estimated the current cooling demand of the Netherlands. To project the cooling demand until 2050, we used three different adoption scenarios of electric cooling systems. Afterwards, two separate analyses were done. On the one hand, we simulated the IEEE 906-bus European Network on Python to evaluate the effect residential cooling would on the voltage in a low-voltage distribution network for different adoption scenarios and ownership percentages. On the other hand, we simulated the Dutch energy market during a heat wave using the software Plexos©, analysing the changes in energy price and revenue of solar and battery energy storage systems.

1.3. Case study

This work addresses two challenges produced by residential E-cooling: congestion on the distribution networks and changes in the overall energy market. Thus, this section provides the conditions considered for each case, including the method used to estimate the Dutch country-wide cooling demand.

1.3.1. Cooling demand in The Netherlands

We considered four different types of residential buildings for our E-cooling model: stand-alone houses, semi-detached houses, terraced houses and apartments. All are considered to have different building parameters. In addition, we considered if the terraced houses are in the corner or middle of the building. To account for the different characteristics per type of house, we first determined the dimensions of the houses. Then, the average k-value and c-value of the houses are determined from the respective building type. Later, we estimated the infiltration rate for each type of building was determined. Finally, the resulting thermal load was translated into electric demand by using a heat pump controlled by a thermostat.

The surface area of the buildings was determined using demographic information from [23,24]. The information available provides an overview of the number and area per house type. To avoid simulating every house, we evaluated the distribution of area per house type and used the mean value to create a representative area per house type. The dimensions of the buildings are then estimated from the surface area. The surface area (per floor), n_{stories}, is determined from the dimensions of the building together with the thickness of the walls using

$$A = \left(W - 2 \cdot d_{\text{wall}}\right) \cdot \left(L - 2 \cdot d_{\text{wall}}\right) \cdot n_{\text{stories}}\,, \tag{1}$$

Table 1
Parameters used for each building type.

Parameter	Stand-alone	Semi-detached	Terraced	Apartment	Units
Surface area	190	144	127	88	m^2
Amount of stories	3	3	2	1	–
Length	10	9	10	12	m
Width	7	6	7	8	m
Height	9	9	6	3	m
WWR	0.3	0.3	0.3	0.4	–
Window area front/back	18.9	16.2	12.6	9.6	m^2
Window area sides	27	24.3	–	–	m^2
R-value window [26]	0.39	0.5	0.48	0.55	m^2K/W
R-value wall [26]	1.66	2.42	2.45	2.72	m^2K/W
k-value window [26]	0.13	0.1	0.1	0.09	W/(K-m)
k-value wall [26]	0.12	0.08	0.08	0.07	W/(K-m)
c-value window [26]	58	45	47	41	W/(kg-K)
c-value wall [26]	240	165	163	147	W/(kg-K)
Infiltration rate [27][a]	0.5	0.4	0.42/0.4	0.39	$dm^3/(s\text{-}m^2)$
Conditioning percentage[a]	20	26	23/26	46	%
HP thermal power[a]	9.3	7.0	6.0/5.1	3.6	kW

[a] The values are given for the corner and middle house, respectively.

where W and L are the width and length of the house, and the wall thickness d_{wall} is assumed to be 20 cm. Stand-alone and semi-detached houses are both assumed to have three stories, while terraced apartments are assumed to have two and one story, respectively. A single story is assumed to have a height of 3 m, from which the height of all types of buildings can be determined. Similarly, it is assumed that not all the house is heated simultaneously, so a conditioning percentage was considered per building type. The window surface area for each type of building was estimated by assuming a commonly used assumption for the window-to-wall ratio (WWR). Usually, the WWR is assumed to be around 0.3 in the Netherlands [25]. In this model, the assumption is also used except for apartment buildings where a slightly higher WWR is assumed due to the low amount of bare walls and the subsequent need for more natural light from the remaining bare walls. Since not all exterior walls have windows; the WWR is applied only to exterior walls that are assumed to have windows. For all types of buildings, it is assumed that the roof does not have windows. All other walls that are not shared by a neighbouring house are assumed to have windows except the side walls for terraced houses and apartments. An overview of all dimensions of each type of building and window area can be seen in Table 1.

The k-value and c-value were then determined from [23]. The construction year of the building often gives an indication of the materials used for walls and windows and the types of layout for the walls and windows (i.e., cavity walls). The construction year was then linked to an average R-value. By linking historic average R-values with building eras, the weighted average R-value of the whole building stock can be estimated per building type [28]. The R-value was then converted into the k-value and c-value according to

$$k = \frac{L_{\text{wall/window}}}{R} \tag{2}$$

and

$$c = \frac{k}{\rho \cdot \alpha} \tag{3}$$

respectively, where L stands for the thickness of the wall or windows. The ρ is the density and the α is the thermal diffusivity of the material. The thermal diffusivity for the windows was taken from [29]. For the walls, a combination of bricks and the insolation material XPS was used to approximate the values for an insulated wall [29]. The resulting k-value and c-value for each type of building are shown in Table 1.

The infiltration rate was then determined for each type of building. The work in [27] provided an extensive study of infiltration rates for Dutch houses. The study was done for 320 Dutch dwellings, including different building types and construction years. The pressurization test at a pressure difference of 10 Pa was used, following the respective technical standards (NEN 2686, NEN-EN 13829 and NEN-EN-ISO 9972). Additional measurements at 50 Pa were also used. For this work, we used the average value of the distributions for the representative building per type. The used values are shown in Table 1. The orientation of the buildings also influences the amount of solar irradiation incident on the building. In this work, we assumed that all houses are oriented straight south (azimuth 0), and all corners have an angle of 90 °, meaning that all other facades face another cardinal direction.

Once the hourly thermal demand is determined, it is converted into electrical demand to simulate its impact on the power market. For this work, we used heat pumps to supply the thermal demand, using the relationship provided by [30] to calculate the HP COP as

$$COP = 3.09 - 0.075 \cdot T_{\text{amb}} + 0.024 \cdot RH\,, \tag{4}$$

where T_{amb} is the ambient temperature and RH is the relative humidity. The ambient temperature was obtained from the KNMI and the RH was assumed to be 85%. In addition, three thermostat operation modes were considered to control the heat pump. First, a

Table 2
Parameters used for each scenario.

Scenario		Heat pump operation mode percentage		
		No constraint	Hard constraint	Soft constraint
Local Independence	(LI)	20	20	60
Stated Pledges	(SP)	20	60	20
Global Transition	(GT)	80	10	10

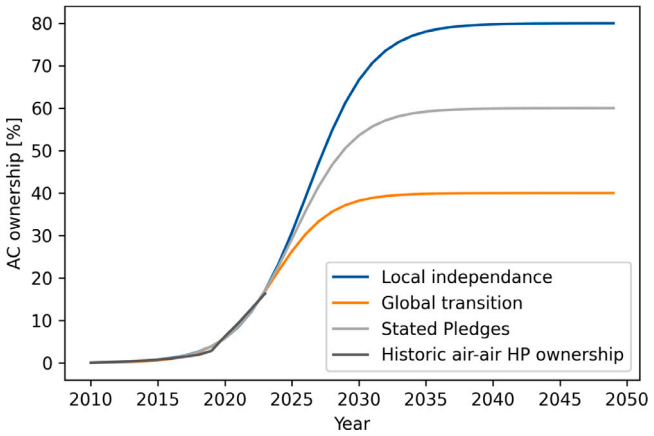

Fig. 2. The three S-curves for the air–air-based heat pump ownership together with the historical ownership.

no constraint mode, where heating or cooling is allowed at any given time during the day. Second, the *hard constraint* mode allows the logic to only heat or cool during the given time slots (in this work, between 7:00 and 9:00 and 17:00 and 22:00). Third, the *soft constraint* mode allows to change the reference temperatures of the logic based on the same time slots; this will cause increased heating or cooling to occur during the time slots and less heating or cooling outside of the time slot. Two reference temperatures are given, a heating reference temperature (18 °C in this work) and a cooling reference temperature (22 °C in this work). For the soft constraints two more reference temperatures are added to the logic, 15 °C for heating and 24 °C for cooling.

Three different scenarios were considered for the simulations, based on the ENTSO-E's 10-year network development plan (TYNDP) and different consumer-based energy market forecasts. The *Stated Pledges* (SP) scenario gives a business-as-usual outlook, following the current Dutch energy transition adoption trends. The *Local Independence* (LI) scenario gives a distributed, country-wide individual-based system, to achieve carbon neutrality by 2050 and at least reduce carbon emissions by 55% by 2030 but assuming that the import of energy on the European continent is not allowed, relying instead on the willingness of local initiatives to achieve a global goal. The *Global Transition* (GT) scenario gives the opposite view from Local Independence with a unified and cooperative European energy network. However, this scenario is based on economies of scale and aims to achieve these goals by investing in centralized low-carbon solutions that allow for the imports of energy on the European continent. All scenarios assume net zero carbon emissions in 2050 and would adhere to the 1.5 °C climate-warming Paris Climate Accord. The projected adoption of heat pumps for cooling ($AC\%$) associated with those scenarios until 2050 is 60%, 80% and 40%, respectively, as shown in Fig. 2, which is given by

$$AC\% = \frac{\text{Sat}}{1 + e^{-k\cdot(x-x_0)}}, \tag{5}$$

where Sat is the expected saturation adoption by 2050, k is the slope coefficient that defines the steepness of the curve, x_0 is the year corresponding to the midpoint of the S-curve, and x is the year of interest. The adoption scenarios considered by Eneco consider that, as the technology is maturing, its adoption rate is higher thanks to favourable policies and decreasing prices, rapidly increasing the ownership. After some time, the adoption rate decreases to a relatively stable ownership condition. Table 2 provides the final distribution of operation modes per each scenario, considering the ownership projections shown in Fig. 2. Similarly, to account for the temperature increase over the projected period, we considered a linear yearly increase in temperature, from 2012 to 2050 of 1.5 °C.

1.3.2. Low-voltage distribution network

The effect on the local low-voltage grid is determined by simulating the IEEE low-voltage three-phase grid in Python using Power Pandas. The IEEE low-voltage grid is a standardized European residential grid rated at 416 V serviced by a 0.8 MVA medium-voltage to low-voltage transformer [31,32]. The grid consists of 906 buses and 55 standardized single-phase loads, to which the E-cooling demand is added. All buses, loads and lines contain geographical information that results in the grid shown in Fig. 3(a). An example of the standard load for residential homes without E-cooling in the IEEE grid can be observed in Fig. 3(b). The cooling demand

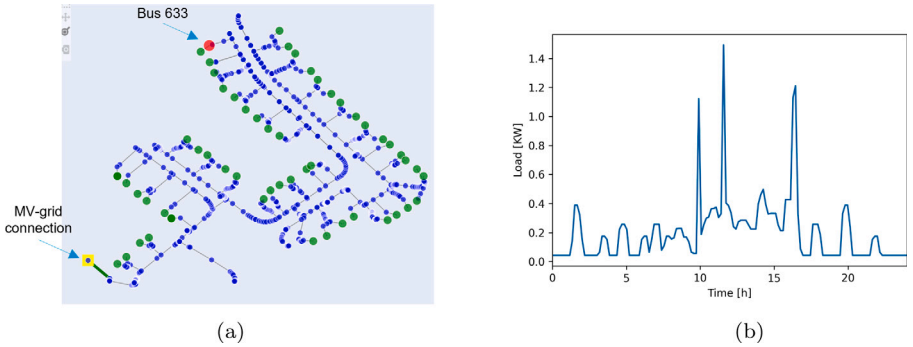

Fig. 3. a. Layout of the IEEE 906-bus low-voltage network, b. An example of the standard IEEE residential loads (load 39).

is summed with the standard load; the average cooling demand of all types of buildings is taken. Depending on the heat pump ownership percentage of the simulation, the cooling demand is only added to randomly chosen loads. We considered an uniform random selection function from Python.

Then, solar generation is added randomly to 30% of the load buses (using the same selection function as the HP adoption), based on the current Dutch residential PV adoption [33]. The average amount of installed photovoltaic (PV) modules per household is 10 to 12 [34]; in this work, we considered that every household has 12 modules. Each module is assumed to have a rated power of 315 W per (the characteristics for a single panel were obtained from [35]), and data from the Royal Dutch Meteorological Institute was used to calculate the PV power production [36].

The grid is simulated for one heat wave in 2020 between the 4th and 10th of August. The seven days are simulated with 10 min intervals in order to test compliance with EN50160 regulations. The European standard states, among others, that the 10-min interval RMS voltage magnitude cannot variate more than 10% for 95% of the measured intervals for the total of the low-voltage and medium-voltage grid [37]. Usually, this means that the low-voltage part of the grid is responsible for half of the variation, so it cannot deviate more than 5% for 95% of the time. In addition to this, the voltage magnitude can never drop more than 15% according to EN50160 [37].

1.3.3. Dutch energy market

We considered the number of buildings per building type to scale the cooling demand from individual homes to the national level. The Dutch Central Bureau of Statistics (CBS) provides data on current building stock by type. However, this data set reflects the current situation and does not account for potential future growth in building stock. To address this, the growth in the number of buildings was linked to projected population growth in the Netherlands. The CBS also offers population growth estimates for the coming decades. By dividing the current building stock by the current population, the number of buildings per inhabitant was calculated. Then, this ratio was applied annually, multiplying it by the expected population growth to estimate the expansion of the building stock for each building type in future years. Finally, to calculate the national residential cooling demand, the individual cooling demand per building type is multiplied by the ownership percentage of air-to-air-based heat pumps and the building stock of each building type for that year. This yields the total annual cooling demand for each type of building. By adding the cooling demand across all types of buildings, the total nationwide residential cooling demand is obtained.

After the physical effects of the cooling demand were determined, the direct economic effect was determined. The simulations were done during a heat wave between the 13th and 20th of August. To estimate the country-wide cooling demand, simulations of the different types of buildings where done, based on demographic information available on the type and number of such buildings in the country. The simulations of the Dutch energy market were performed in the software Plexos©, excluding the effect of the neighbouring countries. The specific years selected for the simulation are 2026, 2028, 2030, 2035, 2040, and 2050. Furthermore, the cooling demand varies over the years, depending on the scenario being simulated. Plexos© is not able to input the electric cooling demand directly; therefore, a participation factor, calculated as the inverse of the COP, is used to calculate the electric energy consumed to supply the E-cooling demand and sum it to the base demand.

Two different analyses were performed: the market price influences and the asset revenue influences. First, the market price is investigated using the hourly day-ahead market price, and the prices are ranked for every simulation to determine the influence of cooling on market prices. Next, 30% of the cooling demand is removed from the model and readded as a flexible demand source. The software is capable of dispatching the demand automatically in the most price-optimal way. The analysis is then repeated for the flexible cooling to compare the base-case static cooling and flexible cooling market prices with the no-cooling simulation. Second, the revenues for different sustainable generation technologies are investigated, and the difference in revenue compared to the scenario without cooling was determined to uncover whether the business cases of certain technologies change with the introduction of cooling. Asset revenue was specifically looked at for the simulated week. The revenue of each asset was then compared with that of the base case without any cooling.

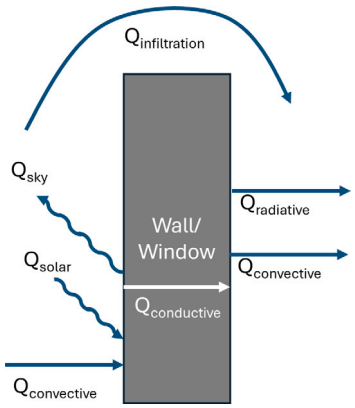

Fig. 4. An overview of the heat balance of a wall/window, with all heat flows shown used in the simulations.

Table 3
Equations used for the heat transfer coefficients.

Parameter	Symbol	Equation
Radiative heat transfer coefficient	h_{rad}	$= \epsilon \cdot \sigma \cdot \left(T_1^2 + T_2^2\right) \cdot \left(T_1 + T_2\right)$
Sky temperature (Swinbank model)	T_{sky}	$= \left[\left(9.284 \cdot e^{-6} \cdot T_{\text{amb}}^2\right)^{0.25}\right] \cdot T_{\text{amb}}$
Conductive heat transfer coefficient	h_{cond}	$= \frac{k}{L}$
Convective heat transfer coefficient (McAdam model)	h_{conv}	$= \begin{cases} 5.7 + 3.8 \cdot v & \text{if} \quad v < 5 \\ 6.47 + v^{0.78} & \text{if} \quad v \geq 5 \end{cases}$

2. Buildings thermodynamic modelling

The heat transfer mechanisms considered for the thermodynamic model of a house are shown in Fig. 4. This means that the cavity walls of double- or triple-glazed windows are not thermodynamically modelled during the simulations, but we calculated the k-values and c-values for double- and triple-glazed windows. The simplification assumption is made to reduce the simulations' computational cost. In addition, the average of the k-value and c-value were taken for each type of building. All energy streams are added to each other to determine the net heat transfer. The temperatures of all windows and walls are determined individually per side of the building, and the temperature on the outside and inside is determined via the heat balance. This way, the overall heat balance for the inside and outside of the window or wall is, respectively

$$T_{\text{out,i}} = T_{\text{out,(i-1)}} + \frac{\Delta t \cdot A}{m \cdot c} \cdot \left[\alpha \cdot G + h_{\text{conv}} \cdot \left(T_{\text{amb}} - T_{\text{out,(i-1)}}\right) + h_{\text{rad,out}} \cdot \left(T_{\text{sky}} - T_{\text{out,(i-1)}}\right) + h_{\text{cond}} \cdot \left(T_{\text{in,(i-1)}} - T_{\text{out,(i-1)}}\right)\right] \tag{6}$$

$$T_{\text{in,i}} = T_{\text{in,(i-1)}} + \frac{\Delta t \cdot A}{m \cdot c} \cdot \left[h_{\text{cond}} \cdot \left(T_{\text{out,(i-1)}} - T_{\text{in,(i-1)}}\right) + h_{\text{conv,in}} \cdot \left(T_{\text{inside,(i-1)}} - T_{\text{in,(i-1)}}\right) + h_{\text{rad,in}} \cdot \left(T_{\text{inside,(i-1)}} - T_{\text{in,(i-1)}}\right)\right] \tag{7}$$

The heat transfer coefficients are calculated using the correlations described in [10], and summarized in Table 3. The indoor temperature of the house T_{inside} is obtained from the preceding calculation step and the ambient temperature T_{amb} is obtained using the Royal Dutch Meteorological Institute (KNMI) weather data for the current time step. In these equations, T_{in} and T_{out}, are the internal and external surface temperature of the walls, respectively, T_{sky} is the sky temperature, Δt denotes the time interval between consecutive steps (in seconds), A represents the surface area of the object, m is its mass and c denotes its specific heat capacity (in [J/(kg K)]). Furthermore, α and G represent the absorptivity of the object and the solar irradiance on its surface, respectively. Also, ϵ is the emissivity, σ is the Stefan–Boltzmann constant, k is the material conductivity, L is the with of the wall, window or roof and v is the wind speed. h_{cond}, h_{conv} and h_{rad} are the conductive, convective and radiative heat transfer coefficients.

The internal temperature of the wall and windows then influence the heat transfer that flows into the building. Thus, the heat flow into the building is

$$Q_{\text{internal,i}} = A \cdot \Delta t \cdot \left[h_{\text{conv,in}} \cdot \left(T_{\text{in,(i-1)}} - T_{\text{inside,(i-1)}}\right) + h_{\text{rad,in}} \cdot \left(T_{\text{in,(i-1)}} - T_{\text{inside,(i-1)}}\right)\right] \tag{8}$$

the value is then added to the equations for the inside temperature shown in (9). In the equation, the heat transfer coefficients hold as in the calculation for the internal surface temperature.

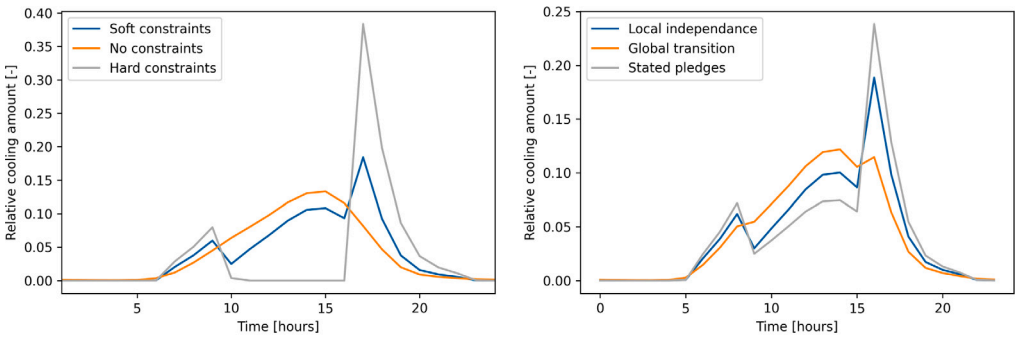

Fig. 5. (a): The resulting daily pattern of the three thermostat operation modes. (b): The resulting daily pattern of the three scenarios.

Residential buildings have internal heat sources. The occupants and heat generation appliances like stoves, ovens and incandescent lighting increase the temperature indoors. We assumed houses with highly efficient appliances, induction cooking and LED lighting; thus, internal heat gains can be neglected in this case [38].

The final equation for the heat transfer effects is shown in Eq. (9). As explained, the three different sources of heat transfer are summarized. After this, it is divided by the volumetric heat capacity c_{air} [J/(m^{3}K)] times the volume of the inside air (V_{air}). The resulting amount is the temperature change compared to the last time step; thus, this is then added to the temperature of the previous time step.

$$T_{ins,i} = T_{ins,i\text{-}1} + \frac{Q_{window} + Q_{wall} + Q_{solar}}{V_{air} \cdot c_{air}}$$
$$T_{ins,i} = T_{ins,i\text{-}1} + \frac{Q_{window} + Q_{wall} + A_{window} \cdot I_{solar} \cdot \tau^2}{V_{air} \cdot c_{air}} \quad (9)$$

where T_{ins} is the instantaneous indoor temperature, Q_{window}, Q_{wall} and Q_{solar} represent the thermal energy provided from the windows, walls and solar irradiance, respectively, A_{window} is the area of the window, I_{solar} is the irradiance, τ is the window transmittance

3. Results and discussion

3.1. Cooling demand in The Netherlands

To extrapolate the cooling demand to the future, one must determine the hourly demand profile for the reference year. As mentioned, this was done by combining the different thermostat operation modes for each scenario, as shown in Table 2. These ratios were chosen to reflect the underlying idea of each scenario. The resulting daily patterns corresponding to each mode are shown in Fig. 5(a). The hard-constraint mode, which aligns with current gas boiler trends, does not exhibit cooling demand outside of given cooling periods. However, it experiences a significant spike in usage during peak load times, as is currently common; this will put a strain on the grid. Opposed to this, the hourly pattern of no-constraint shows a parabolic-like distribution throughout the middle of the day, when usually renewable generation is at its highest. The no-constraint mode can be expected to generate less strain on the grid and could be seen as a form of demand-side response because of this. Finally, the soft constraint mode shows a mixture between both the aforementioned results, as it is allowed to have some cooling during the day; a lower parabolic-like pattern is observed, and a lower demand peak during peak loads is observed. The resulting hourly patterns of the scenario types are shown in Fig. 5(b). As illustrated, the Stated Pledges scenario has the largest spike in demand, as this scenario reflects the business-as-usual situation in the future. The Global Transition shows a pattern with the least strain on the grid as a society-oriented change is aimed at in this scenario.

We projected the cooling demand for 2024 to 2050 for each type of building separately and then summed to the yearly cooling demand. The determined annual thermal cooling demands for each type of building are shown in Fig. 6(a). As can be observed, the stand-alone houses consume around double the amount of cooling than the next building type, semi-detached houses. The double consumption of stand-alone buildings is due to the large exposed surface area of the building and the high infiltration rate. In addition, the insulation values of the stand-alone buildings are slightly worse than the other types of buildings. Finally, the overall size of the building is also larger than any of the other types of buildings. All of the aforementioned reasons cause significantly higher cooling demand in stand-alone houses. In addition, the increasing trend in the graph indicates the increase in temperature due to climate change. The weather data has rising temperatures until 2050, as explained before. The weather data has a linear increase in temperature until a global increase in temperature of 1.5 °C is reached in 2050 compared to 2012.

To determine the country-wide cooling demand, we scaled up the model built in previous steps. Two scaling factors are taken into account as explained in Section 1.3.1. The air–air-based heat pump ownership percentages over the years, and the number and

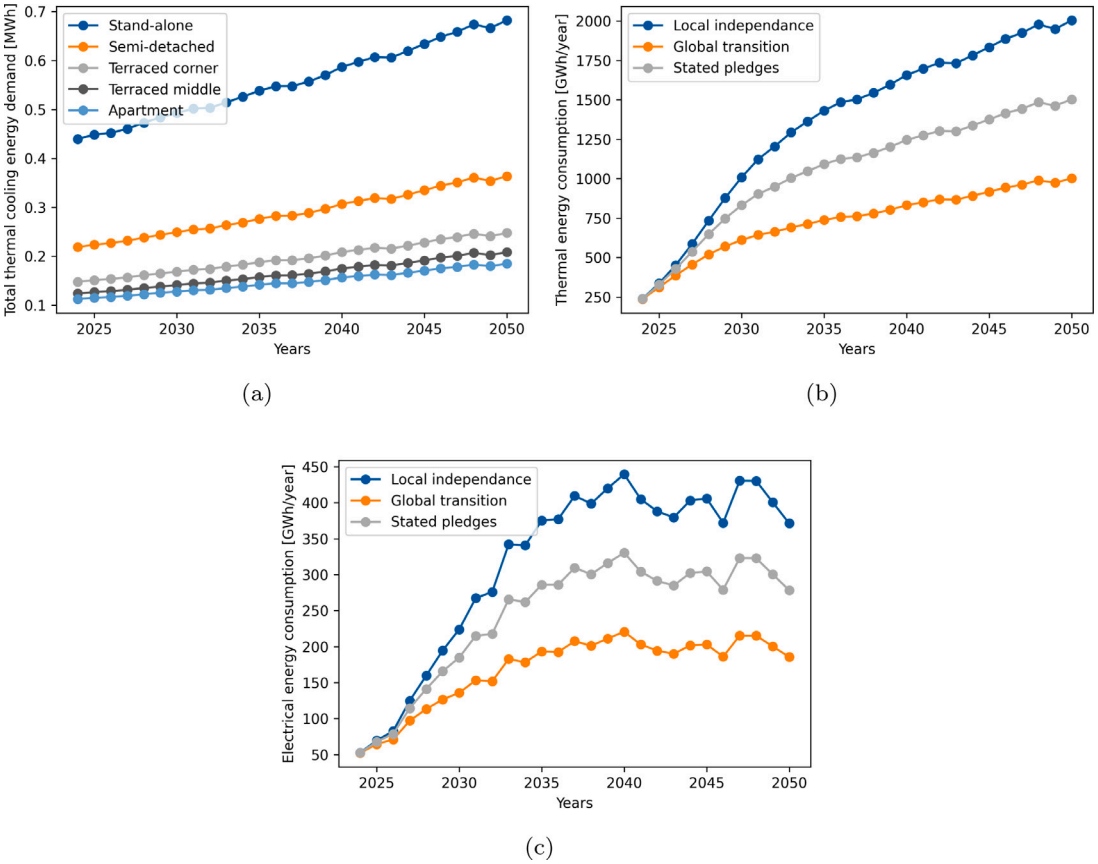

Fig. 6. (a): The total yearly thermal cooling demand per house type for an individual house between 2024–2050. (b): The total yearly thermal cooling demand per scenario between 2024–2050. (c): The total yearly electric cooling demand per scenario between 2024–2050.

growth of buildings in the Netherlands. The total thermal demand for each scenario until 2050 is demonstrated in Fig. 6(b). A steep initial growth is observed until the mid-2030s, mainly due to the rapid adoption of air–air-based heat pumps, as shown in Fig. 2. After this period, the main growth seen in the graph is due to the growth of the building stock and the growing cooling demand per household due to climate warming. The distinction between the scenarios is caused mainly by the difference in the growth of air–air-based heat pump ownerships. In the S-curves, the saturation value for each scenario is different, causing a different final yearly thermal cooling demand for each scenario.

To determine the electric cooling demand from the thermal cooling demand, the hourly thermal demand was divided by the hourly COP. The final yearly electric cooling demand can be observed per scenario in Fig. 6(c). The electric demand follows a pattern similar to the thermal demand shown before. With a strong increase until the mid-2030s and a plateau after for each scenario. Nevertheless, an observable difference between the thermal demand and the electric demand is the fluctuations in demand in the last 15-year period. The fluctuations were most likely caused by the temperature fluctuations over the year, yielding slightly different results. In addition, the final electric demand was based on the hourly thermal and COP demand, whereas the thermal demand was based on daily demand. This would increase the fluctuations in demand on a daily basis influencing the yearly total demand.

The final electric cooling demand for the highest scenario (Local Independence) resulted in an electric demand of around 0.4 TWh/year after 2035. The only other report that estimates the Dutch residential cooling demand, estimates around 1.1 TWh/year in 2030 [4], so this work lies lower. Furthermore, total electricity use in 2020 in the Netherlands amounted to 108 TWh/year, according to CBS. The cooling demand seems to be insignificant compared to the overall electricity demand. However, the cooling demand is erratic and unpredictable. The daily contributions of the cooling demand can go up to 2.5% of the annual demand, which is approximately 10 GWh on a single day compared to 300 GWh of the average country-wide daily electricity demand.

3.2. Low-voltage distribution network

After determining the magnitude of the cooling demand, the effects of cooling on the physical grid, particularly in the voltage stability, were investigated. The IEEE 906-bus European LV network was then simulated for the heat wave week for all scenarios and heat pump ownership percentages. The root mean square (RMS) voltage magnitude was recovered for the 10 min intervals from

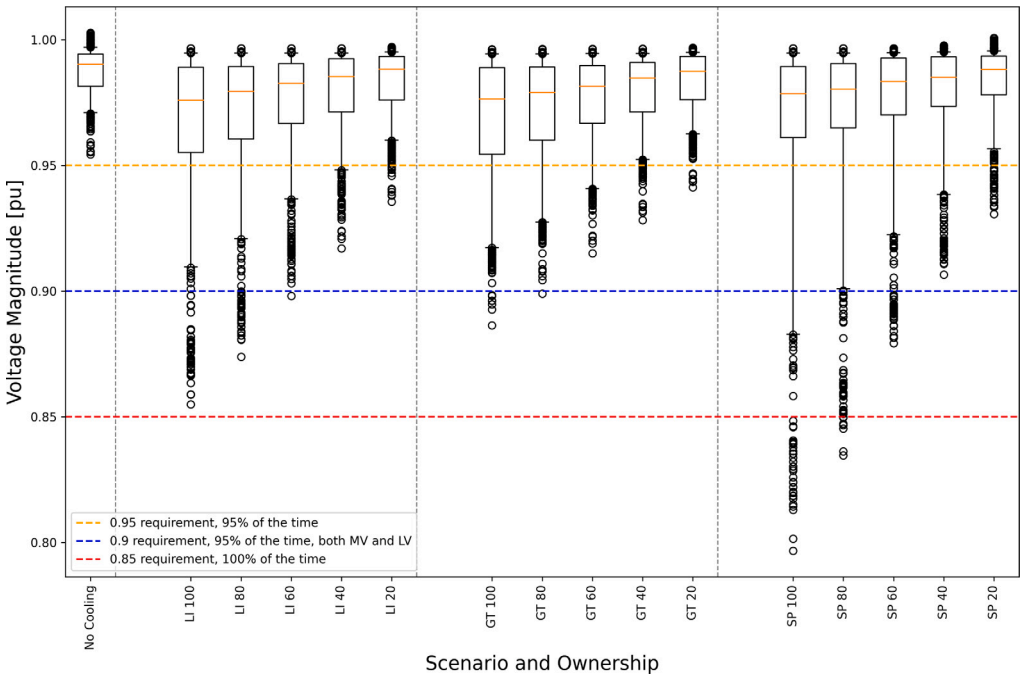

Fig. 7. A box-plot distribution of the voltage magnitude in bus 633 in per unit values for different scenarios and heat pump ownership percentages (LI = Local Independence, GT = Global Transition, SP = Stated Pledges).

the lowest voltage magnitude bus. Bus 633 is the bus with the lowest voltages in the low-voltage grid; therefore, it was chosen for the analysis. The voltage magnitudes are plotted for the entire week for the 10 min intervals in Fig. 7. The whiskers of the box plot are then set at 95% of the samples to easily see whether the grid adheres to the EN50160 regulations, while providing an overview of the spread of the voltage magnitude.

The base case without any cooling shows clear adherence to European regulations. For all remaining simulations with cooling, the power quality deteriorates visibly, and the spread increases downwards and has more outliers. The increase in spread is due to the increase in peak demand as a result of cooling demands. As can be seen, increasing ownership of heat pumps for each scenario drastically reduces the voltage in the network. The increase in the percentage of ownership of heat pumps causes greater peak demand as more households have a heat pump that they will use simultaneously. There appears to be a linear correlation between the spread and ownership, this was expected as total demand is also linear over the heat pump ownership rate.

Only four simulations fully adhere to the EN50160 regulations and would not transgress any of the power quality regulations. The simulations fully adhering to the EN50160 regulations are all the lowest ownership percentages and the 40% ownership percentage for the Global Transition (GT) scenario. The lower ownership percentages have a lower total demand as there are fewer heat pumps present in the grid; thus, the grid does not get oversaturated. The Global Transition scenario has the most favourable hourly pattern; the pattern follows the solar generation pattern relatively well and thus utilizes a large part of the locally generated solar power directly without interacting with the medium-voltage grid. On the other hand, the two highest ownership simulations for the Stated Pledges scenario, do not adhere to any of the voltage-magnitude rules of the EN50160 regulations. In these simulations, the residential circuit would be disconnected from the medium-voltage grid to protect the overall grid. This would mean power outages would occur in the neighbourhood, which could have large implications for residents and the components of the grid. For the remaining nine simulations, the grid partially adheres to the EN50160 regulations. The outliers do not exceed the 15% rule of the power quality regulations, but the whiskers of the boxplot do exceed the 5% deviation limit. However, the deviation of over 5% for more than 5% of the intervals could be compensated by the medium voltage grid, since the total deviation is allowed to be 10%. However, this would mean that there needs to be more flexibility in the medium-voltage grid, which might not be feasible at the given time.

Simulations with partial adherence will, therefore, put heavy restrictions on the medium-voltage network as the total deviation of 10% cannot be exceeded. This will increase the demand for flexibility in the medium-voltage grid, or require upgrades to the low-voltage infrastructure. For instance, the medium-voltage grid could ask for lower demand by its users in other low-voltage networks or direct connections to consumers in their network. In addition, the low-voltage grid could increase the number of connections it has to the medium-voltage grid to increase the overall power supply capacity of the grid. Finally, the low-voltage grid itself could be upgraded to increase the capacity of the grid. All of the above solutions would have an economic cost, increasing the network cost, and thus would have indirect economic effects on the power market. The partial adherence to European power quality regulations and, thus, the economic effects are seen in ownership rates from 40% onward, as explained before. The expected

ownership percentages for each scenario based on historical data are shown in Fig. 2. However, historical data shows that the current ownership rate is already just below 20% and is increasing fast. Therefore, it is likely that the ownership percentage of 40% is reached and that the indirect economic effects that this entails will occur if no alternatives are implemented.

3.3. Dutch energy market

The direct economic effects of the cooling demand are now investigated. The Dutch grid is simulated in Plexos© for one week during a heatwave in summer. This licenced software allows market simulations at large scale. We used historical and forecasted energy price information, together with a grid model of the Dutch power system. The data was provided by Eneco. The total hourly market prices of the simulations were calculated using no cooling demand, a static cooling demand and a 30% flexible cooling demand. Finally, the business cases of different sustainable generation and storage sources are investigated to determine how this would change under increasing cooling demand. The Dutch grid was simulated for eight years distributed between 2026 and 2050 for the three scenarios (resulting in 24 cases), where the cooling demand increases over the years according to the overall yearly demand of the model presented in Section 1.3.1. The resulting market prices were ranked by increasing prices for the simulated week and analysed.

We grouped the results into three categories: price increase, no change in price, and price decrease. A representative price-duration plot for each category found for the market-ranked prices is presented in Fig. 8. These plots allow one to determine the time a determined range of prices persisted during a certain period. The steep changes mean sudden changes in energy price, without intermediate pricing during the week. Using Fig. 8(b) as example, approximately 110 h of the 168 h during the week, the energy price was below 25 €/MWh, then around 15 h had a price between 25 €/MWh and 200 €/MWh, and the reminder 43 h had prices above 200 €/MWh.

The results show that 15 out of the 24 cases had a market price increase, 6 out of the 24 cases showed no difference, and only 3 of the 24 cases showed a price decrease in the overall market price compared to the base case. The increase in prices was expected because when the demand for electricity increases, the price should also increase, as shown in Fig. 8(a). The middle price range corresponds to the current peak prices when a cooling demand is expected to occur. In most cases, the electricity price in the middle price range increased; although high prices can be expected at night for the future energy market because less sustainable energy generation will take place during the night. No significant differences in market prices can be observed between the base case and the cooling cases in Fig. 8(b). This is due to the fact that the cooling demand is not significant enough in these simulations to increase the marginal price in the system.

A decrease in market prices can be observed when cooling is applied to the system in Fig. 8(c). The decrease in market prices is mainly observed for the high peak prices that the model expects at night or in the late evening. The decrease is caused by the Plexos© optimization methodology. Due to the slow ramp constraints of several other flexible demands in the system, the flexible demand did not scale down on time in the no-cooling case, as the system does not optimize ahead of time and only reacts to the current price. In cases with cooling demand, the cooling demand during the day forced the other flexible demands to scale down their demand ahead of peak prices, resulting in less demand during peak prices and a decrease in price. However, the decrease in market prices is not realistic for real-life applications, as most flexible demand industries will look ahead of time at what the market prices will do and will respond on time.

In addition, no significant differences can be observed between having only static cooling and the 30% flexible cooling scenario in almost every simulation. There is no significant difference between both cooling scenarios due to the relatively fast ramping constraints of flexible cooling demand and the relatively low amount of flexible cooling of the overall cooling demand. On the one hand, the high ramp rate in cooling causes Plexos© to dispatch the cooling demand at times when there is little or no difference in market price to keep the network cost equal. As cooling demand in residents is relatively fast in ramping up and down cooling demand, this cannot be decreased. On the other hand, the relatively low amount of flexible cooling of 30% in the system of the overall cooling demand results in very few differences between both cooling scenarios, as not enough cooling is removed to change marginal prices. The share of flexible cooling cannot be increased, as this would counteract the scenarios which envision the dispatch of cooling demand during a certain time period.

Next, the influence of the cooling demand on solar generation and battery storage was investigated. The simulation with Plexos©, also provides information on the market participation of different generation assets. The changes are based on the demand–supply conditions during the simulations, in this case, as a result of adding the residential e-cooling loads created by the different scenarios. The revenue per assets was determined and showed in Fig. 9. In this analysis, only static cooling was considered, as no significant influence between flexible and static demand was found.

The difference in revenue for the solar power generation and battery capacity on a utility scale is presented in Fig. 9. There is a clear increase in revenue of up to 100% visible for the solar energy revenue. Especially in the Local Independence (LI) and in the Stated Pledges (ST) scenarios a significant increase is observed. The increase in solar revenue is due to the overlap in time between solar energy generation and cooling demand. This decreases the curtailment of solar energy and thus increases the amount of solar energy used. Also, in some of the scenarios, there is a price increase in general, as explained. This would also cause an increase in revenue for solar plants.

In the battery revenue graph, a decrease in revenue is seen in most simulations. The decrease in battery revenue is most likely due to the network having fewer energy surpluses because of the higher demand during the day, when usually high generation occurs. In the base case, energy surpluses in the system could be absorbed by the battery. As the battery is charged less than in the base case, it is also not able to sell as much energy, decreasing its revenue. The business case for solar energy seems thus to become

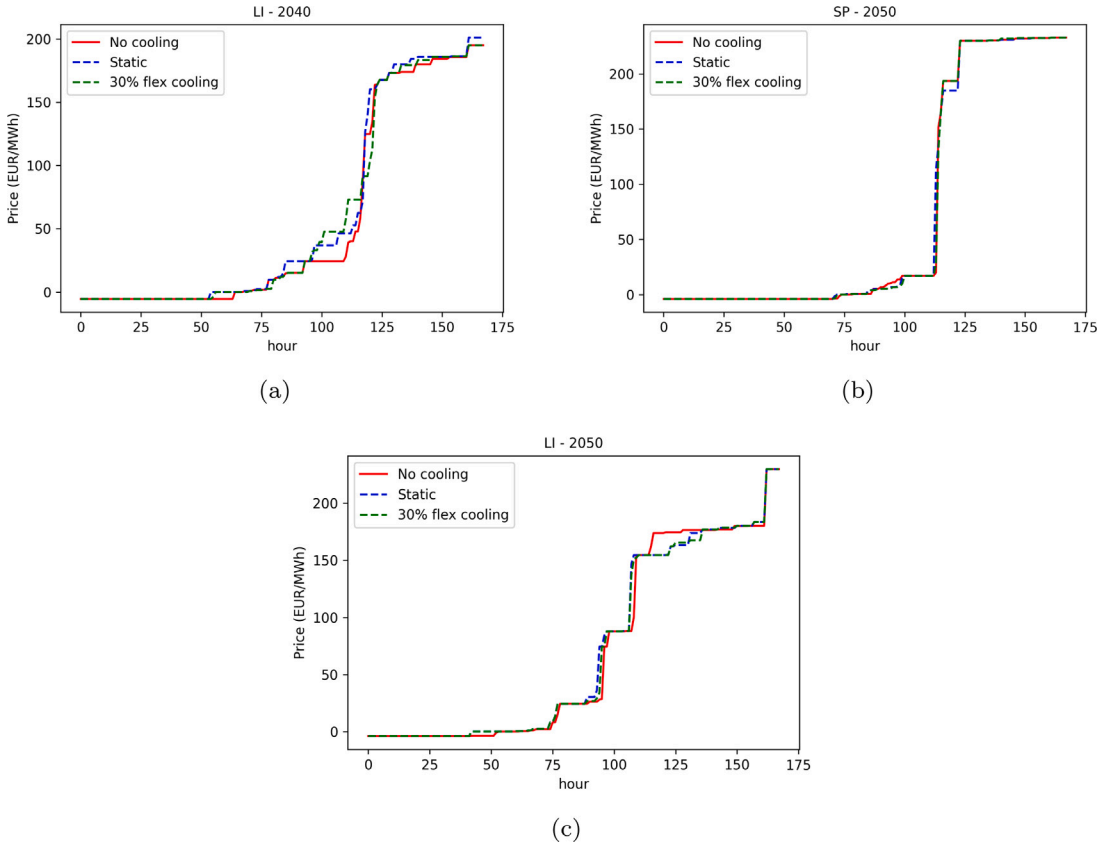

Fig. 8. The ranked prices for a representative case with (a) a price increase, (b) no change in price, and (c) a price decrease.

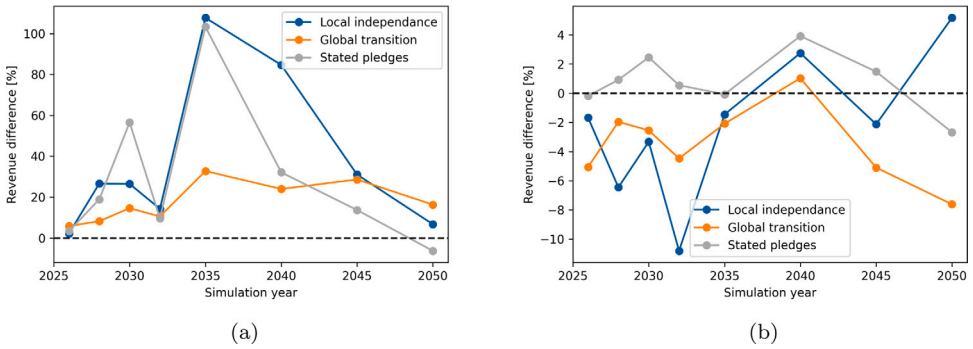

Fig. 9. The asset revenue difference between no cooling and static cooling added to the grid for (a) solar generation and (b) battery storage.

more interesting as revenue increases, while the business case for batteries becomes slightly worse. However, this was only tested in one heat wave week for several years; the sample size is not very large. Further, a lot of differences between the simulations are present, which are not known as each scenario has its own assumptions in the Plexos© model with a different energy mix. Thus, it is not evident to draw a final conclusion from this analysis.

4. Conclusions

This paper used a thermodynamic model to determine the magnitude and pattern of residential cooling based on fundamental heat flows through the average Dutch residential house, and projected it until 2050. The effects of E-cooling were then tested in the IEE 906-bus European Network to determine the effect of growing power demand on the low-voltage distribution system. Finally, a model of the Dutch energy market was used to study also the effect of E-cooling on the energy prices. Our main conclusions are as follows:

- The consumption of cooling demand in the residential sector consists of spatial cooling to increase thermal comfort. Due to the energy transition, increasing the amount of heat pumps and the warming of the climate change, the magnitude of cooling demand will increase substantially.
- The final nationwide cooling energy demand amounted to between 0.2 TWh and 0.4 TWh annually in 2050, depending on the scenario. Despite the annual cooling demand being a relatively small part of the overall electricity consumption in the Netherlands (currently 108 TWh), it was shown how daily contributions of residential cooling can amount to 2.5% of the yearly cooling demand on a single day, causing undervoltages in distribution networks and price changes in the energy market.
- The addition of cooling demand showed a significant impact on the power quality of the low-voltage network. For heat pump ownerships from 40% and above, the regulations could partially not be abided by. For the Global Transition scenario, the hourly pattern decreased the influence of cooling, while the Stated Pledges hourly pattern worsened the power quality of the grid, indicating the opportunity of demand side response for E-cooling. To compensate for this challenge, DSOs are opting for grid reinforcement, which will ultimately lead to increased energy prices.
- The energy market analysis showed an increase in the market price for 15 of the 24 cases, and no major price difference was observed for the remaining nine simulations. Furthermore, the addition of flexible cooling demand of 30% of the total cooling demand, which Plexos© automatically dispatched, did not produce a difference in market price.
- In the revenue analysis of sustainable generation assets, solar generation showed a strong increase in revenue when E-cooling was present because the generation and thermal demand peaks aligned; thus, less curtailment was required. Also, a decrease of up to 10% in revenue was observed for utility-scale batteries for the same simulations. The decrease in revenue was attributed to the decrease in excess energy in the grid during the week as the demand rose, this lowered the amount of available energy for the batteries hindering the opportunity to sell energy during energy shortages.

In addition, we have the following recommendations for future research based on this work:

- **Reduce data limitations in the thermodynamic model:** Weather data limitations were shown to have a large impact on the final cooling demand. More complex weather predictions could address this challenge.
- **Model the evolution of insulation values:** We assumed insulation values in the thermodynamic model would remain constant; it is, however, expected that an increasing trend in insulation improvement will occur in the Netherlands. Thus, studies in predicting such changes would provide better input data for our model.
- **The addition of home energy storage solutions in the physical grid simulations:** Only residential loads and rooftop PV panels are incorporated in the simulations. However, EVs and home storage solutions, either electric or thermal, become more common and could have an impact on the results.
- **Grid composition optimization:** The grid composition remains equal for each simulation. It could be expected, however, that in reality, due to the change in the business case for some generation assets, the grid composition could change to address this and other challenges caused by the energy transition. Thus, future work should study the required engineering and financial aspects of such changes.

CRediT authorship contribution statement

Jim de Wind: Writing – original draft, Software, Methodology, Investigation, Formal analysis, Conceptualization. **Joel Alpízar-Castillo:** Writing – review & editing, Writing – original draft, Validation, Supervision, Software, Project administration, Formal analysis. **Julian Visser:** Validation, Data curation. **Laura Ramírez-Elizondo:** Supervision, Funding acquisition.

Declaration of competing interest

The authors declare the following financial interests/personal relationships which may be considered as potential competing interests: Laura Ramirez-Elizondo reports financial support was provided by Netherlands Enterprise Agency. If there are other authors, they declare that they have no known competing financial interests or personal relationships that could have appeared to influence the work reported in this paper.

Acknowledgements

The project was carried out with a Top Sector Energy subsidy from the Ministry of Economic Affairs and Climate, carried out by the Netherlands Enterprise Agency (RVO). The specific subsidy for this project concerns the MOOI subsidy round 2020. In addition, Eneco provided a model of the Dutch grid and weather data for the market simulations.

Data availability

The data that has been used is confidential.

References

[1] Koninklijk Nederlands Meteorologisch Instituut, Klimaatstreepjescode - warming stripes, 2020, URL: https://www.knmi.nl/over-het-knmi/nieuws/klimaatstreepjescode-warming-stripes.

[2] Centraal Bureau voor de Statistiek, Energieverbruik van particuliere huishoudens, 2018, URL: https://www.cbs.nl/nl-nl/achtergrond/2018/14/energieverbruik-van-particuliere-huishoudens.

[3] Centraal Bureau voor de Statistiek, Warmtepompen; aantallen, thermisch vermogen en energiestromen, 2024, URL: https://opendata.cbs.nl/#/CBS/nl/dataset/85523NED/table.

[4] V. Rovers, Schatting van de elektriciteitsvraag van airconditioners in nederlandse woningen, 2024, URL: https://publications.tno.nl/publication/34643172/0QzXXhpm/TNO-2024-R11165.pdf.

[5] M. Jakubcionis, J. Carlsson, Estimation of European union residential sector space cooling potential, Energy Policy 101 (2017) 225–235, http://dx.doi.org/10.1016/j.enpol.2016.11.047.

[6] M.D. Rosa, V. Bianco, F. Scarpa, L.A. Tagliafico, Heating and cooling building energy demand evaluation; a simplified model and a modified degree days approach, Appl. Energy 128 (2014) 217–229, http://dx.doi.org/10.1016/j.apenergy.2014.04.067.

[7] L.D. Harvey, Using modified multiple heating-degree-day (HDD) and cooling-degree-day (CDD) indices to estimate building heating and cooling loads, Energy Build. 229 (2020) http://dx.doi.org/10.1016/j.enbuild.2020.110475.

[8] Atlas leefomgeving, Stedelijk hitte-eiland effect (UHI), 2023, URL: https://www.atlasleefomgeving.nl/stedelijk-hitte-eiland-effect-uhi.

[9] D. Choi, C. Kim, A data-driven approach to discover hidden complicated relationships of energy variables and estimate energy consumption in U.S. homes, Build. Environ. 267 (2025) 112175, http://dx.doi.org/10.1016/j.buildenv.2024.112175, URL: https://www.sciencedirect.com/science/article/pii/S0360132324010175.

[10] J. Alpízar-Castillo, L.M. Ramírez-Elizondo, P. Bauer, Modelling and evaluating different multi-carrier energy system configurations for a dutch house, Appl. Energy 364 (2024) http://dx.doi.org/10.1016/j.apenergy.2024.123197.

[11] J. Ahn, J.S.H. and, Origins of whole-building energy simulations for high-performance commercial buildings: Contributions of the 1975 ASHRAE algorithms for heat balance-based hourly heating and cooling load calculations, Sci. Technol. Built Environ. 31 (3) (2025) 327–340, http://dx.doi.org/10.1080/23744731.2024.2446002, arXiv:https://doi.org/10.1080/23744731.2024.2446002.

[12] P. Zhao, D. Cao, W. Hu, Y. Huang, M. Hao, Q. Huang, Z. Chen, Geometric loss-enabled complex neural network for multi-energy load forecasting in integrated energy systems, IEEE Trans. Power Syst. 39 (4) (2024) 5659–5671, http://dx.doi.org/10.1109/TPWRS.2023.3345328.

[13] H. Chen, H. Huang, Y. Zheng, B. Yang, A load forecasting approach for integrated energy systems based on aggregation hybrid modal decomposition and combined model, Appl. Energy 375 (2024) 124166, http://dx.doi.org/10.1016/j.apenergy.2024.124166, URL: https://www.sciencedirect.com/science/article/pii/S0306261924015496.

[14] J. Ye, F. Luo, J. Cao, L. Yang, Day ahead load forecasting of integrated energy system based on multi-model combination, in: International Conference on Computer Application and Information Security, ICCAIS 2021, 12260, 2022, http://dx.doi.org/10.1117/12.2637374, URL: https://www.spiedigitallibrary.org/conference-proceedings-of-spie/12260/2637374/Day-ahead-load-forecasting-of-integrated-energy-system-based-on/10.1117/12.2637374.full,

[15] G. Zhu, Y. Gao, H. Liu, Optimal scheduling of an integrated energy system considering carbon trading mechanism and multi-energy supply uncertainties in a real-time price environment, Sustain. Energy Grids Netw. 38 (2024) 101351, http://dx.doi.org/10.1016/j.segan.2024.101351, URL: https://www.sciencedirect.com/science/article/pii/S2352467724000808.

[16] Z. Wang, Y. Hao, G. Zhao, M. Wang, Z. Su, J. Zhang, Day-ahead optimal dispatch method of integrated electric-heat-cool-gas energy system based on N-1 safety criterion, Energy Build. 323 (2024) 114800, http://dx.doi.org/10.1016/j.enbuild.2024.114800, URL: https://www.sciencedirect.com/science/article/pii/S0378778824009162.

[17] O.S. Acosta, P. Mandal, T. Senjyu, Offsetting commercial structure electric cooling loads – technical analysis using grid connected PV, in: 2023 IEEE Industry Applications Society Annual Meeting, IAS, 2023, pp. 1–14, http://dx.doi.org/10.1109/IAS54024.2023.10406369.

[18] J. Alpízar-Castillo, L. Ramírez-Elizondo, A. van Voorden, P. Bauer, Aggregated residential multi-carrier energy storage as voltage control provider in low-voltage distribution networks, (ISSN: 0306-2619) 2025, http://dx.doi.org/10.2139/ssrn.5174336, URL: https://ssrn.com/abstract=5174336.

[19] J. Lersch, R. Tang, M. Weibelzahl, J. Weissflog, Z. Wu, Assessing the impacts of energy sharing on low voltage distribution networks: Insights into electrification and electricity pricing in Germany, Appl. Energy 378 (2025) 124743, http://dx.doi.org/10.1016/j.apenergy.2024.124743, URL: https://www.sciencedirect.com/science/article/pii/S0306261924021263.

[20] M. Kilthau, V. Henkel, L.P. Wagner, F. Gehlhoff, A. Fay, A decentralized optimization approach for scalable agent-based energy dispatch and congestion management, Appl. Energy 377 (2025) 124606, http://dx.doi.org/10.1016/j.apenergy.2024.124606, URL: https://www.sciencedirect.com/science/article/pii/S0306261924019895.

[21] X. Kan, L. Reichenberg, F. Hedenus, The impacts of the electricity demand pattern on electricity system cost and the electricity supply mix: A comprehensive modeling analysis for europe, Energy 235 (2021) 121329, http://dx.doi.org/10.1016/j.energy.2021.121329, URL: https://www.sciencedirect.com/science/article/pii/S0360544221015772.

[22] M. Waite, E. Cohen, H. Torbey, M. Piccirilli, Y. Tian, V. Modi, Global trends in urban electricity demands for cooling and heating, Energy 127 (2017) 786–802, http://dx.doi.org/10.1016/j.energy.2017.03.095, URL: https://www.sciencedirect.com/science/article/pii/S0360544217304784.

[23] Funda, Find houses and apartments for sale/rent in the netherlands, 2024, URL: www.funda.nl. (Accessed 18 July 2024).

[24] Centraal Bureau voor de Statistiek, The Netherlands in Numbers, CBS, 2023, URL: https://longreads.cbs.nl/the-netherlands-in-numbers-2023/how-many-housing-units-are-there/.

[25] M. Taleghani, M. Tenpierik, A. van den Dobbelsteen, R. de Dear, Energy use impact of and thermal comfort in different urban block types in the netherlands, Energy Build. 67 (2013) 166–175, http://dx.doi.org/10.1016/j.enbuild.2013.08.024, URL: https://www.sciencedirect.com/science/article/pii/S0378778813005215.

[26] M. Ozel, Thermal performance and optimum insulation thickness of building walls with different structure materials, Appl. Therm. Eng. 31 (17) (2011) 3854–3863, http://dx.doi.org/10.1016/j.applthermaleng.2011.07.033, SET 2010 Special Issue, URL: https://www.sciencedirect.com/science/article/pii/S1359431111003929.

[27] C.N. Bramiana, A.G. Entrop, J.I. Halman, Relationships between building characteristics and airtightness of dutch dwellings, in: Energy Procedia, 96, Elsevier Ltd, 2016, pp. 580–591, http://dx.doi.org/10.1016/j.egypro.2016.09.103.

[28] F. van Kuijeren, To see how your house is insulated by the year of construction, 2022, URL: https://vkmakelaars.nl/en/blog/architectural/to-see-how-your-house-is-insulated-by-the-year-of-construction/.

[29] M. Ozel, Thermal performance and optimum insulation thickness of building walls with different structure materials, Appl. Therm. Eng. 31 (17) (2011) 3854–3863, http://dx.doi.org/10.1016/j.applthermaleng.2011.07.033, SET 2010 Special Issue, URL: https://www.sciencedirect.com/science/article/pii/S1359431111003929.

[30] M.N. Izham, T.M.I. Mahlia, Effect of ambient temperature and relative humidity on COP of a split room air conditioner, 2010, URL: www.uniten.edu.my/jee.

[31] PandaPower, 3-phase grid data, 2024, URL: https://pandapower.readthedocs.io/en/latest/networks/3phase_grids.html.

[32] K.P. Schneider, B.A. Mather, B.C. Pal, C.-W. Ten, G.J. Shirek, H. Zhu, J.C. Fuller, J.L.R. Pereira, L.F. Ochoa, L.R. de Araujo, R.C. Dugan, S. Matthias, S. Paudyal, T.E. McDermott, W. Kersting, Analytic considerations and design basis for the IEEE distribution test feeders, IEEE Trans. Power Syst. 33 (3) (2018) 3181–3188, http://dx.doi.org/10.1109/TPWRS.2017.2760011.

[33] DutchNews, One in three dutch homes now have solar panels, but growth slows, 2024, URL: https://www.dutchnews.nl/2024/01/one-in-three-dutch-homes-now-have-solar-panels-but-growth-slows/.
[34] K. Nivera, Solar panels in the netherlands: the ultimate guide, 2024, URL: https://dutchreview.com/expat/household/solar-panels-in-the-netherlands/.
[35] C. Solar, Kupower HIGH efficiency MONO perc MODULE, 2020, URL: https://www.canadiansolar.com/wp-content/uploads/2020/05/Canadian_Solar-Datasheet-KuPower_CS3K-MS_EN.pdf.
[36] K.N.M. Instituut, Jaar 2020, 2021, URL: https://www.knmi.nl/nederland-nu/klimatologie/maand-en-seizoensoverzichten/2020/jaar.
[37] E.C. for Electrotechnical Standardization, Voltage characteristics of electricity supplied by public electricity network, 2022.
[38] R. American Society of Heating, I.A. Air-Conditioning Engineers, 2021 ASHRAE® Handbook - Fundamentals (SI Edition), American Society of Heating, Refrigerating and Air-Conditioning Engineers, Inc. (ASHRAE), ISBN: 978-1-947192-90-4, 2021, URL: https://app.knovel.com/hotlink/toc/id:kpCK08G9X5/ashrae-handbook-fundamentals/ashrae-handbook-fundamentals.